Provided for non-commercial research and education use.
Not for reproduction, distribution or commercial use.

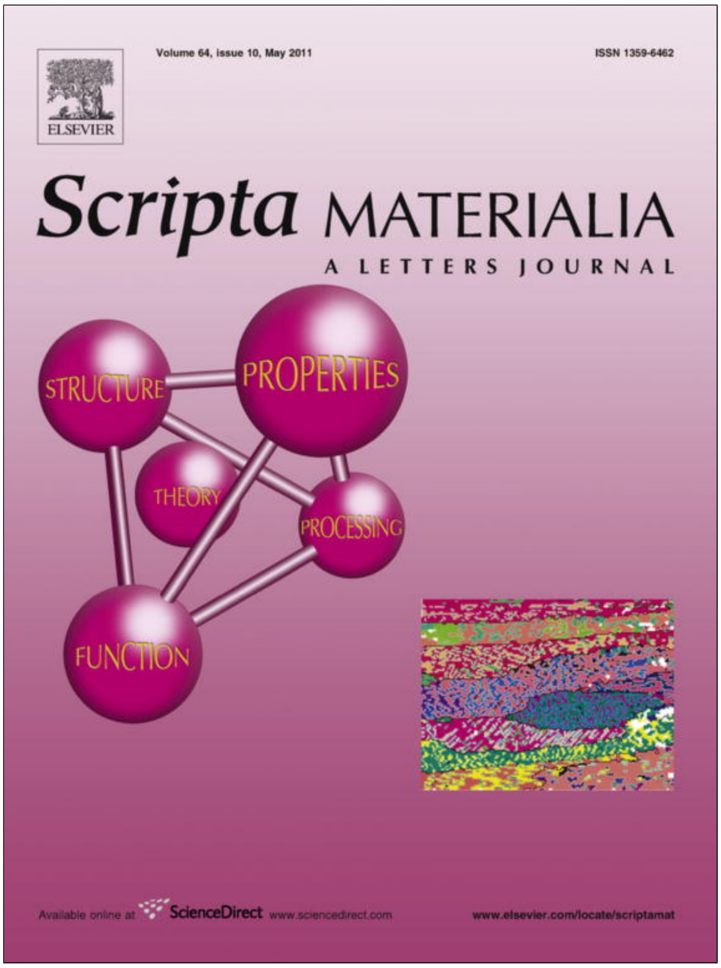
Volume 64, issue 10, May 2011
ISSN 1359-6462
ELSEVIER
Scripta MATERIALIA
A LETTERS JOURNAL
STRUCTURE
PROPERTIES
THEORY
PROCESSING
FUNCTION
Available online at ScienceDirect www.sciencedirect.com
www.elsevier.com/locate/scriptamat

This article appeared in a journal published by Elsevier. The attached copy is furnished to the author for internal non-commercial research and education use, including for instruction at the authors institution and sharing with colleagues.

Other uses, including reproduction and distribution, or selling or licensing copies, or posting to personal, institutional or third party websites are prohibited.

In most cases authors are permitted to post their version of the article (e.g. in Word or Tex form) to their personal website or institutional repository. Authors requiring further information regarding Elsevier's archiving and manuscript policies are encouraged to visit:

http://www.elsevier.com/copyright

Available online at www.sciencedirect.com
ScienceDirect
Scripta Materialia 64 (2011) 978–981
Scripta MATERIALIA
www.elsevier.com/locate/scriptamat

Achieving coherent phase transition in palladium–hydrogen thin films

Stefan Wagner,[a,*] Helmut Uchida,[a] Vladimir Burlaka,[a] Martin Vlach,[b] Marian Vlcek,[b] Frantisek Lukac,[b] Jakub Cizek,[b] Carsten Baehtz,[c] Anthony Bell[d] and Astrid Pundt[a]

[a] *Institute for Materials Physics, University of Göttingen, Germany*
[b] *Faculty of Mathematics and Physics, Charles University in Prague, Czech Republic*
[c] *Institute of Ion Beam Physics and Materials Research, Helmholtz-Zentrum Dresden-Rossendorf, Germany*
[d] *Hamburger Synchrotronstrahlungslabor (HASYLAB), Hamburg, Germany*

Received 21 January 2011; revised 1 February 2011; accepted 5 February 2011
Available online 26 February 2011

The thermodynamics of structural phase transformations in thin films depends on the mechanical stress that can be released by plastic deformation. For thin films below a critical film thickness, plastic deformation is energetically unfavourable: thus, the system stays coherent and stress remains. For PdH_c films less than 22 nm thick, a new situation emerges: while the interfaces between matrix and hydride precipitates remain coherent throughout the complete phase transition, misfit dislocations form between the hydride phase and the substrate.

© 2011 Acta Materialia Inc. Published by Elsevier Ltd. All rights reserved.

Keywords: Palladium; Hydrogen; Thin films; Phase transformations; Coherency

Recently, the impact of mechanical stress on the thermodynamic properties of thin film metal–hydrogen systems has been intensively investigated. When stress is released, the thermodynamic properties of thin films tend towards bulk properties [1–4]. It is also known that when stress remains, the thermodynamics itself changes, differing from conventional thermodynamics in a fundamental way [5]. As the nanostructuring of systems progresses, there is a need for experimental studies of this new thermodynamics – therefore model systems need to be found. Metal–hydrogen systems are promising candidates [6].

During interstitial hydrogen absorption and hydride formation, the host lattice of bulk metals in most cases expands linearly with hydrogen concentration [7]. In contrast, in thin films clamped on elastically hard substrates, lateral expansion is suppressed, resulting in a compressive biaxial stress state with in-plane stresses up to the GPa range [8]. This substrate-related mechanical stress superimposes that developing at interfaces inside of the film, at i.e. grain and phase boundaries [10]. The latter will hereafter be referred to as microstructural stress. In principle, depending on the film's thickness, microstructure and adhesion to the substrate, the mechanical energy stored in the stressed film can be dissipated via different channels of plastic deformation. Stress relaxation can be caused by misfit dislocation formation near the film–substrate interface or misfit dislocation loops forming at the interface of matrix and hydride precipitates [9]. Misfit dislocation formation near the substrate is not necessarily related to hydride formation; it depends on the lattice misfit between film and substrate, and on the film's grain size [12,13]. In metal–hydrogen systems, the misfit is modified by the hydrogen concentration, while the grain size determines the yield strength of the film. Additionally, the film can locally or globally detach from the substrate [14,15].

However, below certain values of critical film thickness these relaxation mechanisms are energetically unfavourable [11,16], and a new state of partial coherency may therefore exist in the case of thin films.

Pd films were sputtered at 673 K on 0.43 mm sapphire (0001) in an ultra-high vacuum chamber with a base pressure of 10^{-10} mbar and an argon sputter gas pressure of 2×10^{-4} mbar. The sputter rate was 1.2–1.6 nm min^{-1}. The surface morphology and the microstructure of the films were investigated by scanning electron microscopy (SEM), X-ray diffraction (XRD) and scanning tunnelling microscopy (STM). STM images were processed with

---

* Corresponding author. E-mail: swagner@ump.gwdg.de

1359-6462/$ - see front matter © 2011 Acta Materialia Inc. Published by Elsevier Ltd. All rights reserved.
doi:10.1016/j.scriptamat.2011.02.004

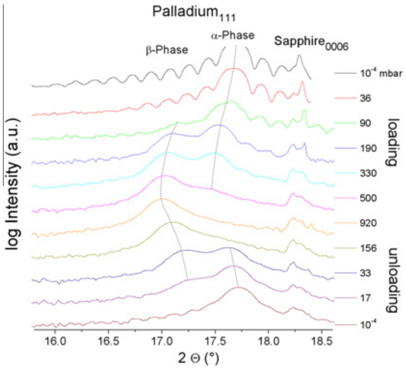

Figure 1. Bragg–Brentano diffraction patterns of 22.5 nm PdH_c on sapphire during the first hydrogen gas loading cycle ($\lambda = 0.68657$ Å). During loading, the Pd (1 1 1) peak shifts to smaller angles, indicating out-of-plane lattice expansion. At $p_{H_2} = 90$ mbar the hydride peak (β-phase) appears. Symmetric to the Pd (1 1 1) peak, thickness fringes occur. During loading, the thickness fringes disappear, but they reappear during subsequent unloading.

WSxM software [17]. The measurements revealed a meander-type film morphology with large domains, but several domain orientations with respect to the substrate. A detailed analysis of the films' microstructure has been published in Ref. [18].

Hydrogen loading of Pd films was performed from the gas phase or electrochemically at room temperature, up to hydrogen concentrations of $c = H/Pd$. Details of the experimental procedure can be found in Ref. [19]. During hydrogen loading, the films' electrical resistance, using the four-point set-up, and their corresponding out-of-plane lattice parameters, were measured in situ at synchrotron radiation facilities at Grenoble (ESRF, Beamline BM 20 operated by the HZDR, Germany) or Hamburg (HASYLAB, Beamline B2 [20]).

Experimental indications for a partially coherent phase transition in thin films are presented in the following. In Fig. 1, PdH_c (1 1 1) diffraction patterns measured in Bragg–Brentano geometry are shown for a 22.5 nm film under hydrogen gas pressures between 10^{-4} and 920 mbar. The upper curve shows the initial PdH_0 (1 1 1) α-phase peak and a sharp (0 0 0 6) sapphire substrate reflection. Symmetrical to the Pd peak, thickness fringes appear, resulting from the interference of photons reflected at the film's surface and the film–substrate interface. Their appearance reveals that the initial film has very smooth interfaces [21].

Fitting the data with the Zolotoyabko model [21,22] for the XRD spectrum of thin crystalline films, the fringes' periodicity and intensity decay involve the film thickness d and a surface lattice disorder parameter, σ; for the current film these have values $d = 22.55(1)$ nm and $\sigma = 0.0042$ nm.[1] During hydrogen loading, the local lattice disorder at the film surface increases, indicated by the reduced numbers and amplitudes of the fringes. At $p_{H2} = 90$ mbar the PdH_c β-phase (hydride) peak appears, while at 920 mbar the film is completely transformed to the hydride phase. During unloading, the film transforms back to the α-phase. Interestingly, the thickness fringes also reappear, indicating that the modifications of the film surface are to a certain extent reversible. However, the amplitude of the fringes remains smaller, with $\sigma = 0.0076$ nm, compared to the initial value.

Fig. 2 shows the lattice parameters of α- and β-phase and the relative resistance R/R_0 of the 22.5 nm Pd film as a function of the hydrogen gas pressure for the first and second loading.

During the first loading, the α-phase lattice parameter a_α and the film resistance only slightly change until the β-phase peak appears at $p_{H_2} = 90$ mbar. At this point, interestingly, the α-phase diffraction peak splits, yielding two discrete a_α values. This can be interpreted in terms of a strained α-matrix locally occurring around the β-precipitates of larger lattice parameter, and a relaxed α-matrix far away from precipitates. During further loading, only the peak related to the strained a_α remains, increasing monotonically until the film is completely hydrided. This increase can be explained by vertical coherent lattice matching between the precipitates and the remaining α-phase, visible in the α-phase reflections.

Fig. 2 also shows that at 90 mbar no change in the resistivity increase occurs. Thus, the onset of precipitation is not visible in the resistivity for 22.5 nm films.

The β-phase lattice parameter a_β increases monotonically with pressure as well, but with a delay between 130 and 190 mbar. The hydrogen concentration at 130 mbar is approximately $c_H \sim 0.11$, as revealed by electrochemical loading of similar films. After unloading, a_α is slightly smaller compared to the initial value ($\Delta a/a = -0.17\%$), and during the second loading it increases monotonically with pressure. The resistance–pressure isotherm is shifted to smaller pressure values. This shows that during the second loading the hydride volume fraction increases faster with hydrogen pressure, indicating an increased hydrogen solubility of the film [19]. The hydride peak appears at the same pressure step, probably caused by the chosen step sequence.

To obtain further insights into the depicted microstructural changes, Fig. 3 shows in addition to the lattice parameters of 22.5 nm Pd, those of 34 nm Pd on sapphire during the initial loading.

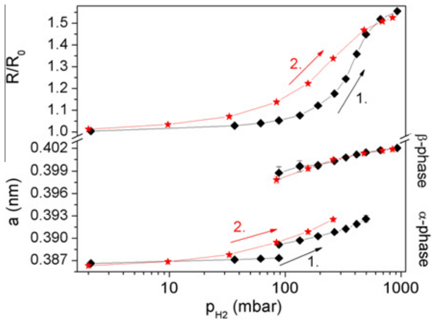

Figure 2. Hydrogen-induced change of lattice parameter a and relative resistance R/R_0 in 22.5 nm Pd on sapphire. The first and second loadings are shown. The hydride phase appears at $p_{H2} = 90\,mbar$ in both loading sequences. The α-phase lattice parameter increases monotonically throughout the complete phase transition, suggesting that hydride precipitates remain coherent with the α-matrix.

---

[1] The films RMS roughness, however, is on the order of 0.3 nm, as revealed by STM (Fig. 4).

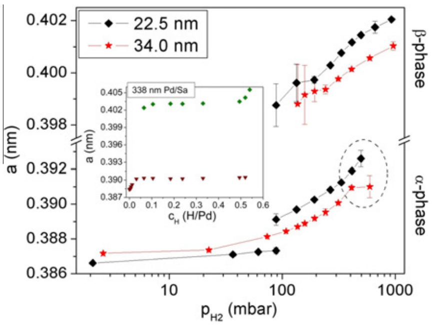

Figure 3. Lattice parameters of 22.5 and 34 nm Pd on sapphire during the first hydrogen gas loading. The phase transition occurs at similar pressures, while the α-phase lattice parameter increments differ significantly between 400 and 600 mbar: a_α of the thicker film stays constant, indicating the loss of coherency between hydride precipitates and matrix. This finding is supported by the figure inset, showing the lattice parameters of 340 nm Pd on sapphire as a function of hydrogen concentration. There, semi-coherent hydrides are formed at an early stage of precipitation – the lattice parameters remain constant almost throughout complete phase transition.

The main information from Fig. 3 is summarized as follows. For the thicker film, a_α initially increases slightly faster with increasing hydrogen pressure, but the corresponding peak does not split at the onset of hydride formation. From this point on, the lattice parameters are systematically smaller for the 34 nm film, revealing that the out-of-plane expansion is smaller for the thicker film. At 130 mbar, a_β of the thicker film retards in similar fashion. Taking the given error bars into account, between 400 and 600 mbar a significant difference in the a_α increments of both films appears. In fact, a_α of the thicker film remains constant during further loading, while a_α of the thinner film continues to increase monotonically. The continuous increase of a_α in 22.5 nm Pd throughout complete phase transition is in accordance with an α-matrix coherently strained by the β-phase precipitates. In contrast, in the 34 nm Pd film the hydride precipitates are interpreted to become semi-coherent towards the α-matrix between 400 mbar (according to $c_H \sim 0.45$ H/Pd) and 600 mbar hydrogen pressure, yielding a constant a_α. Therefore, the critical film thickness for coherent phase transition is below 34 nm, but above 22 nm Pd film thickness.

Consequently, in the case of a very thick 340 nm Pd film on sapphire, the lattice parameters remain constant almost throughout the entire phase transition, see the inset of Fig. 3, verifying semi-coherent hydride formation and stress release in an early stage of precipitation.

The critical thickness of $22\ \text{nm} \leqslant d_{crit}^{\text{Pd}} \leqslant 34\ \text{nm}$ is in good agreement with that of epitaxial NbH_c films on sapphire and the determined $d_{\text{crit}}^{\text{Nb}} = 26.3(2)\ \text{nm}$ [16], taking the line energies W(r) of misfit dislocation loops in Pd and Nb films into account. $W_{\text{Pd}}(r)$ is a factor of 1–2 larger than $W_{\text{Nb}}(r)$ when isotropy or anisotropy of the elastic constants is assumed [16,23], yielding a slightly larger critical thickness in the case of Pd. For GdH_c films on W (1 1 0) the critical thickness is below 12 nm [11].

The partial reversibility of the thickness fringes, as demonstrated in Fig. 1, the different pressure–resistance isotherms during the first and second loadings in Fig. 2, and the delay in the a_β increase at 130 mbar in Fig. 3, however, hint at a certain in-plane stress relaxation present in the 22.5 nm film as well. Interestingly, stress release there only occurs in the β-phase, as it is only visible in the β-reflections. To evaluate the resulting relaxation mechanism, the surface morphology changes in the 22.5 nm Pd film during hydrogen loading were measured in situ by STM. This technique was chosen as STM image analysis is regarded as the best tool for studying the appearance of hydrogen-induced dislocations in thin metal films in situ under true thin film boundary and stress conditions in hydrogen atmospheres above 500 mbar [11,16]. Other methods often used to monitor dislocations, like TEM, require thinned samples with additional surfaces, changing the stress condition from that of the original substrate, especially when hydrogen is needed to be kept in the film.

In Fig. 4 a representative film area of 22.5 nm Pd is shown for the α-phase region ($p_{\text{H}_2} = 55$ mbar, Fig. 4a), after the onset of hydride formation (150 mbar, Fig. 4b) and close to the upper limit of the two-phase field (530 mbar, Fig. 4c), where the film is almost completely hydrided (Fig. 2).

In the α-phase Fig. 4 shows a single domain with looped surface features, bordered by monoatomic steps. These were formed during film growth, resulting from dislocations adjusting for the mismatch between film and substrate [24]. Some faceted, depleted areas 6 nm deep and about 40 nm in diameter are of minor importance here. Comparison of Fig. 4a and b shows that, remarkably, the onset of hydride formation is not directly visible in film topography; the surface features remain unchanged, while the height of the film increases homogeneously by an average of 0.84 nm. This finding is in good agreement with coherent phase precipitation.

At larger pressures, triangular structures appear (Fig. 4c) and the average height increases by another 0.90 nm. The triangles are bordered by atomic glide steps, examples of which are shown in Fig. 4d. As has been shown for Gd and Nb thin films, these steps represent misfit dislocations close to the film–substrate interface (compare Refs. [11,16]). In the case of Pd, dislocation gliding happens at (1 1 1) glide planes, while three of these planes meet the (1 1 1) surface in the ⟨1 1 0⟩ directions, resulting in angles of 60°. This angle was experimentally found in the triangular structures. Thus, for in-plane stress release, dislocations naturally emerge during hydride formation in locally stressed regions, between the hydride and the substrate.

It has been proven for NbH_c thin films that the misfit dislocations are linked to the hydride phase, as the observed large height changes can only be explained by an underlying hydride [16]. However, for the Pd film the surface fraction of the triangular distorted regions is small, even at 530 mbar, where about 80% of the film volume is known to be hydrided (compare Fig. 2). This means that the hydride precipitates are not bordered by the distorted areas, but the triangles appear within the hydrided film area. Further, this means that the interfaces between α- and β-phase are not visible as surface

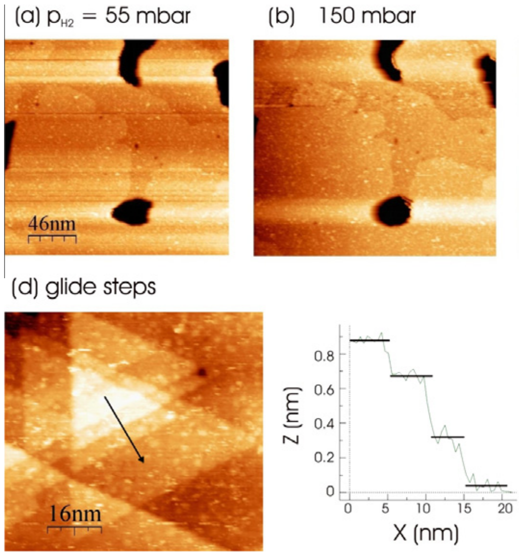

Figure 4. Surface of 22.5 nm Pd on sapphire during hydrogen loading in STM. The as-prepared film surface consists of large domains with looped features of monoatomic steps (α-phase) (a). During initial hydride formation (b), the surface topography remains almost unchanged, but the average height of the surface increases by 0.84 nm. Close to the upper limit of the two-phase-field (c), triangular distorted regions with glide steps occur, representing misfit dislocations formed close to the film–substrate interface. The average step height is 0.28 nm (d), close to the (1 1 1) lattice spacing in Pd hydride (0.23 nm). The arrow indicates the direction of the profile measurement. The small dots are probably related to adsorbates. All pictures were taken in constant current mode, with a gap voltage $U_{Gap} = 1.7$ V and $I = 0.1$ nA.

steps in the STM images. At the phase interfaces the height-signal changes gradually, not in localized steps. This, again, independently supports the interpretation of a fully coherent phase transition for the interfaces between the α-phase and the hydride phase. Therefore, in the 22.5 nm Pd thin film hydride precipitates exist that are coherent with the α-matrix but relaxed towards the substrate. This is a new type of coherency that only can occur in thin films.

The larger overall out-of-plane expansion of the 22.5 nm Pd film compared to the 34 nm film reveals different magnitudes of in-plane stress relaxation. Consequently, for the thicker film the thickness fringes did not reappear during unloading, as more material has been transported to the film surface (not shown here).

In total, a cascade of different critical thickness values for the onset of plastic deformation in PdH_c thin films on sapphire substrates has been found. With increasing film thickness, first the formation of misfit dislocations at the film–substrate interface becomes energetically favourable. These misfit dislocations appear within the hydride precipitates; the hydride phase laterally relaxes, while in the vertical direction it stays coherent with the α-phase matrix. At film thicknesses above about 22 nm, misfit dislocation loop formation around hydride precipitates becomes possible. Above this thickness, the hydride phase relaxes towards the substrate and towards the α-phase. Above 100 nm thickness, films can also detach from the substrate.

As these studies show the existence of a critical thickness, below which hydride precipitates stay coherent with the α-phase matrix throughout complete phase transition in PdH_c thin films on sapphire, a model system to study the thermodynamics of clamped coherent systems has been found.

Financial support of the DFG via projects PU131/7-2 and PU131/9-1, of the Ministry of Education of Czech Republic via MSM0021620834, as well as of the DAAD via D0804229 is gratefully acknowledged. Beam time was kindly provided by HASYLAB (project II-20060117) and HZDR Beamline BM20@ESRF.

[1] S. Wagner, A. Pundt, APL 92 (2008) 051914.
[2] R. Gremaud et al., Acta Mater. 57 (2009) 1209.
[3] Y. Pivak et al., Scripta Mater. 60 (2009) 348.
[4] A. Baldi et al., APL 95 (2009) 071903.
[5] R. Schwarz, A. Khachaturyan, Acta Mater. 54 (2006) 313.
[6] H. Zabel, H. Peisl, PRL 42 (1979) 511.
[7] H. Peisl, G. Alefeld, J. Völkl, Hydrogen in Metals I, Springer Verlag, Berlin, 1978.
[8] A. Pundt, R. Kirchheim, Ann. Rev. Mater. Res. 36 (2006) 555.
[9] U. Laudahn, A. Pundt, et al., JALCOM 293 (1999) 490.
[10] C. Lemier, J. Weissmüller, Acta Mater. 55 (2007) 1241.
[11] A. Pundt et al., PRB 61 (2000) 9964.
[12] A. Pundt, Adv. Eng. Mater. 6 (2004) 11.
[13] W. Nix, Met. Trans. A 20A (1989) 2217.
[14] A. Pundt, E. Nikitin, R. Kirchheim, P. Pekarski, Acta Mater. 52 (2004) 1579.
[15] A. Pundt et al., Scripta Mater. 57 (2007) 889.
[16] K. Nörthemann, A. Pundt, PRB 78 (2008) 014105.
[17] I. Horcas et al., Rev. Sci. Instrum. 78 (2007) 013705.
[18] S. Wagner, A. Pundt, Acta Mat., doi: 10.1016/j.actamat.2010.11.052.
[19] S. Wagner, A. Pundt, Acta Mater. 58 (2010) 1387.
[20] M. Knapp et al., J. Synchrotron. Rad. 11 (2004) 328.
[21] E. Zolotoyabko, J. Appl. Cryst. 31 (1998) 241.
[22] K. Saenger, I. Noyan, JAP 89 (2001) 3125.
[23] D. Sander, Rep. Prog. Phys. 62 (1999) 809.
[24] K. Nörthemann, R. Kirchheim, A. Pundt, JALCOM 356 (2003) 541.